Paper 38

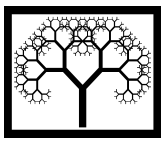

Proceedings of the Seventh International Conference
on Computational Structures Technology,
B.H.V. Topping and C.A. Mota Soares (Editors),
Civil-Comp Press, Stirling, Scotland.

Hybrid Stress-Strain Elements based on the First-Order Single-Layer and Layer-Wise Shell Theories

G.M. Kulikov and S.V. Plotnikova
Department of Applied Mathematics and Mechanics
Tambov State Technical University, Tambov, Russia

Abstract

The exact representation of rigid-body motions in the displacement patterns of the first-order equivalent single-layer (ESL) and layer-wise (LW) shell elements is considered. This consideration requires the development of the strain-displacement relationships of the ESL and LW shell theories with regard to their consistency with rigid-body motions. The fundamental unknowns consist of six displacements of the face surfaces of the shell in the ESL theory and $3(N+1)$ displacements of the face surfaces of layers in the LW shell theory, where N is a number of layers. Such choice of displacements gives the possibility to deduce strain-displacement relationships which are objective, i.e., invariant under rigid-body motions. In order to overcome thickness locking, the simplified material stiffness matrix corresponding to the plane stress state is employed. To overcome shear and membrane locking and have no spurious zero energy modes, the assumed strain and stress resultant fields are invoked. On the basis of this approach a four-node *curved* ESL shell element is designed. The elemental stiffness matrix has six, and only six, zero eigenvalues and requires only direct substitutions. Besides, it is evaluated by using the full exact *analytical* integration.

Keywords: multilayered shell, four-node curved shell element, rigid-body motion.

1 Introduction

One of the main requirements of a finite element that is intended for the general analysis of shells is that it must lead to strain-free modes for rigid-body motions. The adequate representation of rigid-body motions is a necessary condition if an element is to have good accuracy and convergence properties. Therefore, when an inconsistent shell theory is used to construct any finite element, erroneous straining modes under rigid-body motions may appear. This problem has been only studied

for the Kirchhoff-Love shell theory [1-3] and Timoshenko-Mindlin-type shell theory [4, 5]. Herein, first, the more general study on the basis of the first-order equivalent single-layer theory (ESLT) taking into account the transverse normal deformation response is considered. As unknown functions six displacements of the face surfaces of the shell are selected. Secondly, an approach on the basis of the first-order layer-wise theory (LWT) allowing for thickness stretching is also presented. Note that a comprehensive discussion on the use of the LW shell models in engineering applications may be found in books [6, 7] and overview works [8-11]. In our case the fundamental unknowns consist of $3(N+1)$ displacements of the face surfaces of layers [12], where N is a number of layers. Namely such choice of unknowns allowed us to deduce strain-displacement relationships of the ESL and LW shell theories, which are completely free for all rigid-body motions.

It is common knowledge that in some works developing the solid-shell concept [13-16] displacement vectors of the face surfaces are also used and represented in some global Cartesian basis in order to exactly describe rigid-body motions. But in our shell theories selecting as unknowns the displacements of face surfaces of the shell or layers has an another mechanical sense and allows one to formulate any curved ESL or LW shell elements on the basis of the principally new non-linear strain-displacement relationships that are objective, i.e., invariant under all rigid-body motions.

Here, it is developed a refined finite element formulation based on the simple and efficient approximation of ESL shells via four-node *curved* elements [5]. To overcome shear and membrane locking and have no spurious zero energy modes, the assumed strain and stress resultant fields are invoked. In order to circumvent thickness locking the simplified material stiffness matrix [5, 13-15] corresponding to the plane stress state is employed. Taking into account that the displacement vectors of the face surfaces are represented in the *local* reference surface basis, the proposed finite element formulation has substantial computational advantages compared to the conventional isoparametric finite element formulations, since it eliminates the costly numerical integration by deriving the stiffness matrices. Besides, element matrix requires only direct substitutions, i.e., no inversion is needed if sides of the element coincide with lines of principal curvatures of the reference surface and they are evaluated by using the full exact *analytical* integration.

The numerical results demonstrate the efficiency and high accuracy of the developed formulation. For this purpose extensive numerical studies are employed.

2 Problem Formulation

2.1 Preliminaries

Consider a shell built up in the general case by the arbitrary superposition across the wall thickness of N layers of uniform thickness h_k. The kth layer may be defined as a 3D body of volume V_k bounded by two surfaces $S_{k\text{-}1}$ and S_k, located at the distances $\delta_{k\text{-}1}$ and δ_k measured with respect to the reference surface S, and the edge boundary

surface Ω_k (Figure 1). The full edge boundary surface $\Omega = \Omega_1 + \Omega_2 + \ldots + \Omega_N$ is generated by the normals to the reference surface along the bounding curve $\Gamma \subset S$ (with the arc length s) of this surface. It is also assumed that the bounding surfaces S_{k-1} and S_k are continuous, sufficiently smooth and without any singularities. Let the reference surface S be referred to an orthogonal curvilinear coordinate system α_1 and α_2, which coincides with the lines of principal curvatures of its surface; $\mathbf{e}_1$ and $\mathbf{e}_2$ are the tangent unit vectors to the lines of principal curvatures; A_α and k_α are the Lamé coefficients and principal curvatures of the reference surface. The α_3 - axis is oriented along the unit vector $\mathbf{e}_3$ normal to the reference surface.

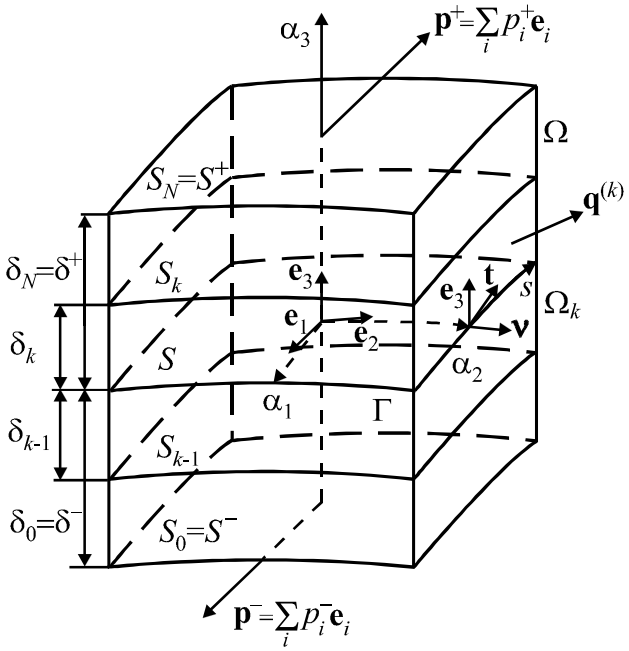

Figure 1: Multilayered shell

The constituent layers of the shell are supposed to be rigidly joined, so that no slip on contact surfaces and no separation of layers can occur. The material of each constituent layer is assumed to be linearly elastic, anisotropic, homogeneous or fiber reinforced, such that in each point there is a single surface of elastic symmetry parallel to the reference surface. Let p_i^- and p_i^+ be the intensities of the external loading acting on the bottom surface $S^- = S_0$ and top surface $S^+ = S_N$ in the α_i coordinate directions, respectively; $\mathbf{q}^{(k)} = q_\nu^{(k)}\boldsymbol{\nu} + q_t^{(k)}\mathbf{t} + q_3^{(k)}\mathbf{e}_3$ are the external loading vector acting on the edge boundary surface Ω_k, where $q_\nu^{(k)}$, $q_t^{(k)}$ and $q_3^{(k)}$ are the components of its vector in the ν, t and α_3 directions; $\boldsymbol{\nu}$ and $\mathbf{t}$ are the normal and tangential unit vectors to the bounding curve Γ. Here and in the following developments the index $k = \overline{1, N}$ identifies the belonging of any quantity to the kth layer; the ab-

breviation $(\,)_{,\alpha}$ implies the partial derivatives with respect to the coordinate α_1 and α_2; indices i, j, ℓ, m take the values 1, 2 and 3; Greek indices α, β, γ, δ take the values 1 and 2.

2.2 ESLT Kinematics

The ESL shell theory is based on the linear approximation of displacements in the thickness direction [17, 18]

$$\mathbf{u} = N^{-}(\alpha_3)\mathbf{v}^{-} + N^{+}(\alpha_3)\mathbf{v}^{+}, \tag{1a}$$

$$\mathbf{u} = \sum_i u_i \mathbf{e}_i, \qquad \mathbf{v}^{\pm} = \sum_i v_i^{\pm} \mathbf{e}_i, \tag{1b}$$

$$N^{-}(\alpha_3) = \frac{1}{h}\left(\delta^{+} - \alpha_3\right), \qquad N^{+}(\alpha_3) = \frac{1}{h}\left(\alpha_3 - \delta^{-}\right), \tag{1c}$$

where $\mathbf{u}$ is the displacement vector; $u_i(\alpha_1, \alpha_2, \alpha_3)$ are the components of this vector; $\mathbf{v}^{\pm}$ are the displacement vectors of surfaces $S^{\pm}$; $v_i^{\pm}(\alpha_1, \alpha_2)$ are the components of these vectors; $N^{\pm}(\alpha_3)$ are the linear shape functions; h is the thickness of the shell. It is important that displacement vectors (1b) are represented in the local reference surface basis $\mathbf{e}_i$ that allows one to eliminate the costly numerical integration by deriving the stiffness matrix.

Substituting displacements (1a) into a vector form of the 3D strain-displacement relationships [5] and replacing Lamé coefficients by their values on the bottom and top surfaces $A_\alpha^{\pm} = A_\alpha\left(1 + k_\alpha \delta^{\pm}\right)$ and middle surface $\overline{A}_\alpha = A_\alpha\left(1 + k_\alpha \overline{\delta}\right)$ in corresponding expressions for the in-plane and transverse shear components, the following equations are obtained:

$$\varepsilon_{\alpha\beta} = N^{-}(\alpha_3) e_{\alpha\beta}^{-} + N^{+}(\alpha_3) e_{\alpha\beta}^{+}, \tag{2a}$$

$$\varepsilon_{\alpha 3} = N^{-}(\alpha_3) e_{\alpha 3}^{-} + N^{+}(\alpha_3) e_{\alpha 3}^{+}, \qquad \varepsilon_{33} = e_{33}. \tag{2b}$$

Here, $e_{\alpha\beta}^{\pm}$ and $e_{\alpha 3}^{\pm}$ are the in-plane and transverse shear components of the strain tensor of face surfaces $S^{\pm}$ defined by

$$2e_{\alpha\beta}^{\pm} = \frac{1}{A_\alpha^{\pm}} \mathbf{v}_{,\alpha}^{\pm} \mathbf{e}_\beta + \frac{1}{A_\beta^{\pm}} \mathbf{v}_{,\beta}^{\pm} \mathbf{e}_\alpha, \tag{3a}$$

$$2e_{\alpha 3}^{\pm} = \frac{A_\alpha^{\pm}}{\overline{A}_\alpha} \boldsymbol{\beta} \mathbf{e}_\alpha + \frac{1}{\overline{A}_\alpha} \mathbf{v}_{,\alpha}^{\pm} \mathbf{e}_3, \qquad e_{33} = \boldsymbol{\beta} \mathbf{e}_3, \tag{3b}$$

$$\boldsymbol{\beta} = \frac{1}{h}\left(\mathbf{v}^{+} - \mathbf{v}^{-}\right), \qquad \overline{\delta} = \frac{1}{2}\left(\delta^{-} + \delta^{+}\right), \tag{3c}$$

where $\overline{\delta}$ is the distance from the reference surface to the middle surface $\overline{S}$. Strain-displacement relationships (2) and (3) are very attractive because they are objective, i.e., invariant under rigid-body motions. It will be discussed in Subsection 2.4.

Using displacements (1) into the strain-displacement equations (3) and allowing for formulas for derivatives of the basis vectors $\mathbf{e}_i$ along coordinate lines [1], we

can write these equations in a scalar form

$$e^{\pm}_{\alpha\alpha} = \frac{1}{\zeta^{\pm}_{\alpha}}\lambda^{\pm}_{\alpha}, \qquad 2e^{\pm}_{12} = \frac{1}{\zeta^{\pm}_{1}}\omega^{\pm}_{1} + \frac{1}{\zeta^{\pm}_{2}}\omega^{\pm}_{2}, \tag{4}$$

$$2e^{\pm}_{\alpha 3} = \frac{\zeta^{\pm}_{\alpha}}{\overline{\zeta}_{\alpha}}\beta_{\alpha} - \frac{1}{\overline{\zeta}_{\alpha}}\theta^{\pm}_{\alpha}, \quad e_{33} = \beta_3,$$

where

$$\lambda^{\pm}_{\alpha} = \left(\frac{1}{A_{\alpha}}v^{\pm}_{\alpha}\right)_{,\alpha} + B_{\alpha\alpha}v^{\pm}_{\alpha} + B_{\alpha\beta}v^{\pm}_{\beta} + k_{\alpha}v^{\pm}_{3}, \quad \omega^{\pm}_{\alpha} = \left(\frac{1}{A_{\alpha}}v^{\pm}_{\beta}\right)_{,\alpha} + B_{\alpha\alpha}v^{\pm}_{\beta} - B_{\alpha\beta}v^{\pm}_{\alpha}, \tag{5}$$

$$\theta^{\pm}_{\alpha} = -\left(\frac{1}{A_{\alpha}}v^{\pm}_{3}\right)_{,\alpha} - B_{\alpha\alpha}v^{\pm}_{3} + k_{\alpha}v^{\pm}_{\alpha}, \qquad \beta_i = \frac{1}{h}\left(v^{+}_{i} - v^{-}_{i}\right),$$

$$\zeta^{\pm}_{\alpha} = 1 + k_{\alpha}\delta^{\pm}, \qquad \overline{\zeta}_{\alpha} = 1 + k_{\alpha}\overline{\delta}, \qquad B_{\gamma\delta} = \frac{1}{A_{\gamma}A_{\delta}}A_{\gamma,\delta} \qquad (\beta \neq \alpha).$$

2.3 LWT Kinematics

The LW shell theory is based on the linear approximation of displacements in the thickness direction of the *k*th layer [12]

$$\mathbf{u}^{(\mathrm{k})} = N^{-}_{k}(\alpha_3)\mathbf{v}^{(\mathrm{k}-1)} + N^{+}_{k}(\alpha_3)\mathbf{v}^{(\mathrm{k})}, \tag{6a}$$

$$\mathbf{u}^{(k)} = \sum_i u^{(k)}_i \mathbf{e}_i, \qquad \mathbf{v}^{(\ell)} = \sum_i v^{(\ell)}_i \mathbf{e}_i \qquad (\ell = k-1, k), \tag{6b}$$

$$N^{-}_{k}(\alpha_3) = \frac{1}{h_k}(\delta_k - \alpha_3), \qquad N^{+}_{k}(\alpha_3) = \frac{1}{h_k}(\alpha_3 - \delta_{k-1}), \tag{6c}$$

where $\mathbf{u}^{(k)}$ is the displacement vector of the *k*th layer; $u^{(k)}_i(\alpha_1, \alpha_2, \alpha_3)$ are the components of this vector; $\mathbf{v}^{(\ell)}$ are the displacement vectors of the face surfaces of the layers; $v^{(\ell)}_i(\alpha_1, \alpha_2)$ are the components of these vectors; $N^{\pm}_{k}(\alpha_3)$ are the linear shape functions of the *k*th layer.

Substituting displacements (6) into the 3D strain-displacement relationships [5] and replacing Lamé coefficients by their values on the bottom and top surfaces $A^{(k-1)}_{\alpha} = A_{\alpha}(1 + k_{\alpha}\delta_{k-1})$ and $A^{(k)}_{\alpha} = A_{\alpha}(1 + k_{\alpha}\delta_k)$, and middle surface $\overline{A}^{(k)}_{\alpha} = A_{\alpha}(1 + k_{\alpha}\overline{\delta}_k)$ of the *k*th layer in corresponding expressions for the in-plane and transverse shear components, one derives

$$\varepsilon^{(k)}_{\alpha\beta} = N^{-}_{k}(\alpha_3)e^{(k-1)}_{\alpha\beta} + N^{+}_{k}(\alpha_3)e^{(k)}_{\alpha\beta}, \tag{7a}$$

$$\varepsilon^{(k)}_{\alpha 3} = N^{-}_{k}(\alpha_3)e^{(k)-}_{\alpha 3} + N^{+}_{k}(\alpha_3)e^{(k)+}_{\alpha 3}, \qquad \varepsilon^{(k)}_{33} = e^{(k)}_{33}, \tag{7b}$$

where

$$2e^{(\ell)}_{\alpha\beta} = \frac{1}{A^{(\ell)}_{\alpha}}\mathbf{v}^{(\ell)}_{,\alpha}\mathbf{e}_{\beta} + \frac{1}{A^{(\ell)}_{\beta}}\mathbf{v}^{(\ell)}_{,\beta}\mathbf{e}_{\alpha} \qquad (\ell = k-1, k), \tag{8a}$$

$$2e_{\alpha 3}^{(k)-}=\frac{A_\alpha^{(k-1)}}{\overline{A}_\alpha^{(k)}}\boldsymbol{\beta}^{(k)}\mathbf{e}_\alpha+\frac{1}{\overline{A}_\alpha^{(k)}}\overline{\mathbf{v}}_{,\alpha}^{(k-1)}\mathbf{e}_3,\qquad 2e_{\alpha 3}^{(k)+}=\frac{A_\alpha^{(k)}}{\overline{A}_\alpha^{(k)}}\boldsymbol{\beta}^{(k)}\mathbf{e}_\alpha+\frac{1}{\overline{A}_\alpha^{(k)}}\overline{\mathbf{v}}_{,\alpha}^{(k)}\mathbf{e}_3, \quad (8b)$$

$$e_{33}^{(k)}=\boldsymbol{\beta}^{(k)}\mathbf{e}_3,$$

$$\boldsymbol{\beta}^{(k)}=\frac{1}{h_k}\left(\mathbf{v}^{(k)}-\mathbf{v}^{(k-1)}\right),\qquad \overline{\delta}_k=\frac{1}{2}\left(\delta_{k\text{-}1}+\delta_k\right). \quad (8c)$$

Note that strain-displacement relationships (7) and (8) are also objective. A proof of this statement is given in the next subsection.

Taking again into account formulas for derivatives of the basis vectors [1] we represent strain-displacement relationships (8) in a scalar form

$$e_{\alpha\alpha}^{(\ell)}=\frac{1}{\zeta_\alpha^{(\ell)}}\lambda_\alpha^{(\ell)},\qquad 2e_{12}^{(\ell)}=\frac{1}{\zeta_1^{(\ell)}}\omega_1^{(\ell)}+\frac{1}{\zeta_2^{(\ell)}}\omega_2^{(\ell)}\qquad (\ell=k-1,k), \quad (9)$$

$$2e_{\alpha 3}^{(k)-}=\frac{\zeta_\alpha^{(k-1)}}{\overline{\zeta}_\alpha^{(k)}}\beta_\alpha^{(k)}-\frac{1}{\overline{\zeta}_\alpha^{(k)}}\theta_\alpha^{(k-1)},\qquad 2e_{\alpha 3}^{(k)+}=\frac{\zeta_\alpha^{(k)}}{\overline{\zeta}_\alpha^{(k)}}\beta_\alpha^{(k)}-\frac{1}{\overline{\zeta}_\alpha^{(k)}}\theta_\alpha^{(k)},\qquad e_{33}^{(k)}=\beta_3^{(k)},$$

where

$$\lambda_\alpha^{(\ell)}=\left(\frac{1}{A_\alpha}v_\alpha^{(\ell)}\right)_{,\alpha}+B_{\alpha\alpha}v_\alpha^{(\ell)}+B_{\alpha\beta}v_\beta^{(\ell)}+k_\alpha v_3^{(\ell)}, \quad (10)$$

$$\omega_\alpha^{(\ell)}=\left(\frac{1}{A_\alpha}v_\beta^{(\ell)}\right)_{,\alpha}+B_{\alpha\alpha}v_\beta^{(\ell)}-B_{\alpha\beta}v_\alpha^{(\ell)}\qquad (\beta\neq\alpha),$$

$$\theta_\alpha^{(\ell)}=-\left(\frac{1}{A_\alpha}v_3^{(\ell)}\right)_{,\alpha}-B_{\alpha\alpha}v_3^{(\ell)}+k_\alpha v_\alpha^{(\ell)},\qquad \beta_i^{(k)}=\frac{1}{h_k}\left(v_i^{(k)}-v_i^{(k-1)}\right),$$

$$\zeta_\alpha^{(\ell)}=1+k_\alpha\delta_\ell,\qquad \overline{\zeta}_\ell^{(k)}=1+k_\alpha\overline{\delta}_k,\qquad B_{\gamma\delta}=\frac{1}{A_\gamma A_\delta}A_{\gamma,\delta}\qquad (\ell=k-1,k).$$

2.4 Rigid-Body Motions

A small rigid-body motion is defined as [1]

$$\mathbf{u}^R=\boldsymbol{\Delta}+\boldsymbol{\Phi}\times\mathbf{R}, \quad (11)$$

$$\mathbf{R}=\mathbf{r}+\alpha_3\mathbf{e}_3,\qquad \boldsymbol{\Delta}=\sum_i\Delta_i\mathbf{e}_i,\qquad \boldsymbol{\Phi}=\sum_i\Phi_i\mathbf{e}_i,$$

where $\mathbf{R}$ is the position vector of any point of the shell; $\mathbf{r}$ is the position vector of any point of the reference surface; $\boldsymbol{\Delta}$ is the constant displacement (translation) vector; $\boldsymbol{\Phi}$ is the constant rotation vector.

In particular, rigid-body motions of the face surfaces of the shell will be

$$\mathbf{v}^{\pm R}=\boldsymbol{\Delta}+\boldsymbol{\Phi}\times\mathbf{R}^\pm,\qquad \mathbf{R}^\pm=\mathbf{r}+\delta^\pm\mathbf{e}_3, \quad (12)$$

where $\mathbf{R}^\pm$ are the position vectors of points of the bottom and top surfaces. The derivatives of the translation and rotation vectors with respect to the curvilinear reference surface coordinates α_1 and α_2 are zero, i.e.,

$$\boldsymbol{\Delta}_{,\alpha}=\mathbf{0},\qquad \boldsymbol{\Phi}_{,\alpha}=\mathbf{0}. \quad (13)$$

By using equations (12) and (13) one can obtain an important expression for derivatives

$$\mathbf{v}_{,\alpha}^{\pm R} = A_{\alpha}^{\pm}\boldsymbol{\Phi}\times\mathbf{e}_{\alpha}. \tag{14}$$

It may be verified by means of equations (12) and (14) that strains given by relationships (2a) and (2b) are all zero in a rigid-body motion, since

$$2e_{\alpha\beta}^{\pm R} = \left(\boldsymbol{\Phi}\times\mathbf{e}_{\alpha}\right)\mathbf{e}_{\beta} + \left(\boldsymbol{\Phi}\times\mathbf{e}_{\beta}\right)\mathbf{e}_{\alpha} = 0,$$

$$2e_{\alpha 3}^{\pm R} = \frac{A_{\alpha}^{\pm}}{\overline{A}_{\alpha}}\left[\left(\boldsymbol{\Phi}\times\mathbf{e}_{3}\right)\mathbf{e}_{\alpha} + \left(\boldsymbol{\Phi}\times\mathbf{e}_{\alpha}\right)\mathbf{e}_{3}\right] = 0, \qquad \varepsilon_{33}^{R} = \left(\boldsymbol{\Phi}\times\mathbf{e}_{3}\right)\mathbf{e}_{3} = 0.$$

So, strain-displacement relationships of the ESL shell theory are invariant under all rigid-body motions.

Further, we represent rigid-body motions of the face surfaces of the *k*th layer as

$$\mathbf{v}^{(\ell)R} = \boldsymbol{\Delta} + \boldsymbol{\Phi}\times\mathbf{R}^{(\ell)}, \qquad \mathbf{R}^{(\ell)} = \mathbf{r} + \delta_{\ell}\mathbf{e}_{3} \qquad \left(\ell = k-1, k\right), \tag{15}$$

where $\mathbf{R}^{(\ell)}$ are the position vectors of the face surfaces of the *k*th layer. Using equations (13) and (15) one derives the following formula for derivatives:

$$\mathbf{v}_{,\alpha}^{(\ell)R} = A_{\alpha}^{(\ell)}\boldsymbol{\Phi}\times\mathbf{e}_{\alpha} \qquad \left(\ell = k-1, k\right). \tag{16}$$

Finally, allowing for equations (15) and (16) we can prove a fundamental statement that strain-displacement relationships of the LW shell theory (7a) and (7b) are also invariant under rigid-body motions, i.e.,

$$\varepsilon_{ij}^{(k)R} = 0.$$

3 Hu-Washizu Variational Equation

It is well known that the Hu-Washizu variational principle provides the basis for derivation of various variational principles, and many different mixed and hybrid finite elements for multilayered shells may be designed. Here and in the following developments, for conciseness, we will consider only one theory, namely, the first-order ESL shell theory which will demonstrate the feature of our approach.

The EST shell theory developed is based on the assumed approximations of displacements (1) and displacement-dependent strains (2) in the thickness direction. Additionally, one should adopt the similar approximation for the assumed displacement-independent strains

$$\varepsilon_{\alpha\beta}^{\mathrm{AS}} = N^{-}\left(\alpha_3\right)E_{\alpha\beta}^{-} + N^{+}\left(\alpha_3\right)E_{\alpha\beta}^{+}, \tag{17a}$$

$$\varepsilon_{\alpha 3}^{\mathrm{AS}} = N^{-}\left(\alpha_3\right)E_{\alpha 3}^{-} + N^{+}\left(\alpha_3\right)E_{\alpha 3}^{+}, \qquad \varepsilon_{33}^{\mathrm{AS}} = E_{33}. \tag{17b}$$

Substituting approximations (1), (3) and (17) into the Hu-Washizu mixed variational principle [19] and accounting for that metrics of all surfaces parallel to the reference surface are identical and equal to the metric of the middle surface, one can derive

$$\iint_{\bar{S}}\left[\left(\mathbf{H}-\mathbf{D}\mathbf{E}\right)^{\mathrm{T}}\delta\mathbf{E} + \left(\mathbf{E}-\mathbf{e}\right)^{\mathrm{T}}\delta\mathbf{H} - \mathbf{H}^{\mathrm{T}}\delta\mathbf{e} + \mathbf{P}^{\mathrm{T}}\delta\mathbf{v}\right]\,\overline{A}_1\overline{A}_2\mathrm{d}\alpha_1\mathrm{d}\alpha_2 \tag{18}$$

$$+\oint_{\overline{\Gamma}}\hat{\mathbf{H}}_{\Gamma}^{\mathrm{T}}\delta\mathbf{v}_{\Gamma}\left(1+k_N\overline{\delta}\right)\mathrm{d}s=0,$$

$$\mathbf{D}=\begin{bmatrix}
D_{1111}^{00} & D_{1111}^{01} & D_{1122}^{00} & D_{1122}^{01} & D_{1112}^{00} & D_{1112}^{01} & 0 & 0 & 0 & 0 & 0\\
D_{1111}^{01} & D_{1111}^{11} & D_{1122}^{01} & D_{1122}^{11} & D_{1112}^{01} & D_{1112}^{11} & 0 & 0 & 0 & 0 & 0\\
D_{2211}^{00} & D_{2211}^{01} & D_{2222}^{00} & D_{2222}^{01} & D_{2212}^{00} & D_{2212}^{01} & 0 & 0 & 0 & 0 & 0\\
D_{2211}^{01} & D_{2211}^{11} & D_{2222}^{01} & D_{2222}^{11} & D_{2212}^{01} & D_{2212}^{11} & 0 & 0 & 0 & 0 & 0\\
D_{1211}^{00} & D_{1211}^{01} & D_{1222}^{00} & D_{1222}^{01} & D_{1212}^{00} & D_{1212}^{01} & 0 & 0 & 0 & 0 & 0\\
D_{1211}^{01} & D_{1211}^{11} & D_{1222}^{01} & D_{1222}^{11} & D_{1212}^{01} & D_{1212}^{11} & 0 & 0 & 0 & 0 & 0\\
0 & 0 & 0 & 0 & 0 & 0 & D_{1313}^{00} & D_{1313}^{01} & D_{1323}^{00} & D_{1323}^{01} & 0\\
0 & 0 & 0 & 0 & 0 & 0 & D_{1313}^{01} & D_{1313}^{11} & D_{1323}^{01} & D_{1323}^{11} & 0\\
0 & 0 & 0 & 0 & 0 & 0 & D_{2313}^{00} & D_{2313}^{01} & D_{2323}^{00} & D_{2323}^{01} & 0\\
0 & 0 & 0 & 0 & 0 & 0 & D_{2313}^{01} & D_{2313}^{11} & D_{2323}^{01} & D_{2323}^{11} & 0\\
0 & 0 & 0 & 0 & 0 & 0 & 0 & 0 & 0 & 0 & D_{3333}
\end{bmatrix}, \quad (19)$$

$$\mathbf{v}=\left[v_1^-\ v_1^+\ v_2^-\ v_2^+\ v_3^-\ v_3^+\right]^{\mathrm{T}},\qquad \mathbf{v}_{\Gamma}=\left[v_{\nu}^-\ v_{\nu}^+\ v_t^-\ v_t^+\ v_3^-\ v_3^+\right]^{\mathrm{T}},$$

$$\mathbf{e}=\left[e_{11}^-\ e_{11}^+\ e_{22}^-\ e_{22}^+\ 2e_{12}^-\ 2e_{12}^+\ 2e_{13}^-\ 2e_{13}^+\ 2e_{23}^-\ 2e_{23}^+\ e_{33}\right]^{\mathrm{T}},$$

$$\mathbf{E}=\left[E_{11}^-\ E_{11}^+\ E_{22}^-\ E_{22}^+\ 2E_{12}^-\ 2E_{12}^+\ 2E_{13}^-\ 2E_{13}^+\ 2E_{23}^-\ 2E_{23}^+\ E_{33}\right]^{\mathrm{T}},$$

$$\mathbf{H}=\left[H_{11}^-\ H_{11}^+\ H_{22}^-\ H_{22}^+\ H_{12}^-\ H_{12}^+\ H_{13}^-\ H_{13}^+\ H_{23}^-\ H_{23}^+\ H_{33}\right]^{\mathrm{T}},$$

$$\hat{\mathbf{H}}_{\Gamma}=\left[\hat{H}_{\nu\nu}^-\ \hat{H}_{\nu\nu}^+\ \hat{H}_{\nu t}^-\ \hat{H}_{\nu t}^+\ \hat{H}_{\nu 3}^-\ \hat{H}_{\nu 3}^+\right]^{\mathrm{T}},\qquad \mathbf{P}=\left[-p_1^-\ \ p_1^+\ -p_2^-\ \ p_2^+\ -p_3^-\ \ p_3^+\right]^{\mathrm{T}}.$$

Here, $D_{\alpha\beta\gamma\delta}^{pq}$, $D_{\alpha 3\beta 3}^{pq}$ and D_{3333} are the components of the constitutive stiffness matrix **D**; $v_{\nu}^{\pm}$, $v_t^{\pm}$ and $v_3^{\pm}$ are the components of the displacement vectors of the face surfaces in the coordinate system ν, t and α_3 (Figure 1); k_N is the normal curvature of the curve Γ; $\overline{\Gamma}$ is the bounding curve of the middle surface; $H_{\alpha\beta}^{\pm}$, $H_{\alpha 3}^{\pm}$ and H_{33} are the stress resultants; $\hat{H}_{\nu\nu}^{\pm}$, $\hat{H}_{\nu t}^{\pm}$ and $\hat{H}_{\nu 3}^{\pm}$ are the load resultants defined as

$$D_{\alpha\beta\gamma\delta}^{pq}=\sum_k n_k^{pq}C_{\alpha\beta\gamma\delta}^{(k)},\qquad D_{\alpha 3\beta 3}^{pq}=\sum_k n_k^{pq}C_{\alpha 3\beta 3}^{(k)},\qquad D_{3333}=\sum_k h_k C_{3333}^{(k)},\qquad (20)$$

$$n_k^{pq}=\int_{\delta_{k-1}}^{\delta_k}\left[N^-\left(\alpha_3\right)\right]^{2-p-q}\left[N^+\left(\alpha_3\right)\right]^{p+q}\mathrm{d}\alpha_3,\qquad \left(p,q=0\text{ and }1\right),$$

$$H_{\alpha\beta}^{\pm}=\sum_k\int_{\delta_{k-1}}^{\delta_k}\sigma_{\alpha\beta}^{(k)}N^{\pm}\left(\alpha_3\right)\mathrm{d}\alpha_3,\qquad H_{\alpha 3}^{\pm}=\sum_k\int_{\delta_{k-1}}^{\delta_k}\sigma_{\alpha 3}^{(k)}N^{\pm}\left(\alpha_3\right)\mathrm{d}\alpha_3,\qquad (21)$$

$$H_{33}=\sum_k\int_{\delta_{k-1}}^{\delta_k}\sigma_{33}^{(k)}\mathrm{d}\alpha_3,\qquad H_{\nu\text{æ}}^{\pm}=\sum_k\int_{\delta_{k-1}}^{\delta_k}q_{\text{æ}}^{(k)}N^{\pm}\left(\alpha_3\right)\mathrm{d}\alpha_3\qquad \left(\text{æ}=\nu,t\text{ and }3\right),$$

where $\sigma_{ij}^{(k)}$ are the stresses of the kth layer; $C_{ij\ell m}^{(k)}$ are the components of the elasticity tensor of the kth layer.

Formulas (20) are valid due to the plane stress enforcement which is done by decoupling the transverse normal stress with all other stresses in the 3D Hooke's law [5, 13-15], i.e., it is supposed that $C^{(k)}_{\alpha\beta 33} = C^{(k)}_{33\alpha\beta} = 0$. This approach may be appreciated as a good remedy for overcoming the thickness locking phenomenon [20].

Further, we write the mixed variational equation (18) for the shell element as

$$\int_{-1}^{1}\int_{-1}^{1}\left[\delta\mathbf{E}^{\mathrm{T}}\left(\mathbf{H}-\mathbf{D}\mathbf{E}\right)+\delta\mathbf{H}^{\mathrm{T}}\left(\mathbf{E}-\mathbf{e}\right)-\delta\mathbf{e}^{\mathrm{T}}\mathbf{H}+\delta\mathbf{v}^{T}\mathbf{P}\right]\overline{A}_1^{e\ell}\overline{A}_2^{e\ell}\mathrm{d}\xi_1\mathrm{d}\xi_2 \qquad (22)$$

$$+\oint_{\overline{\Gamma}^{e\ell}}\delta\mathbf{v}_{\Gamma}^{T}\hat{\mathbf{H}}_{\Gamma}\left(1+k_N\overline{\delta}\right)\mathrm{d}s=0,$$

where $\overline{A}_\gamma^{e\ell}=\overline{A}_\gamma\ell_\gamma^{e\ell}$ are the Lamé coefficients of the middle surface $\overline{S}^{e\ell}$ of the element (Figure 2); $\xi_\gamma=\left(\alpha_\gamma-d_\gamma^{e\ell}\right)/\ell_\gamma^{e\ell}$ are the local curvilinear normalized coordinates; $d_\gamma^{e\ell}=\left(\alpha_\gamma^{-e\ell}+\alpha_\gamma^{+e\ell}\right)/2$ are the coordinates of the center of the element; $2\ell_\gamma^{e\ell}=\alpha_\gamma^{+e\ell}-\alpha_\gamma^{-e\ell}$ are the lengths of the element; $\overline{\Gamma}^{e\ell}\subset\overline{S}^{e\ell}$ is the bounding curve of the element.

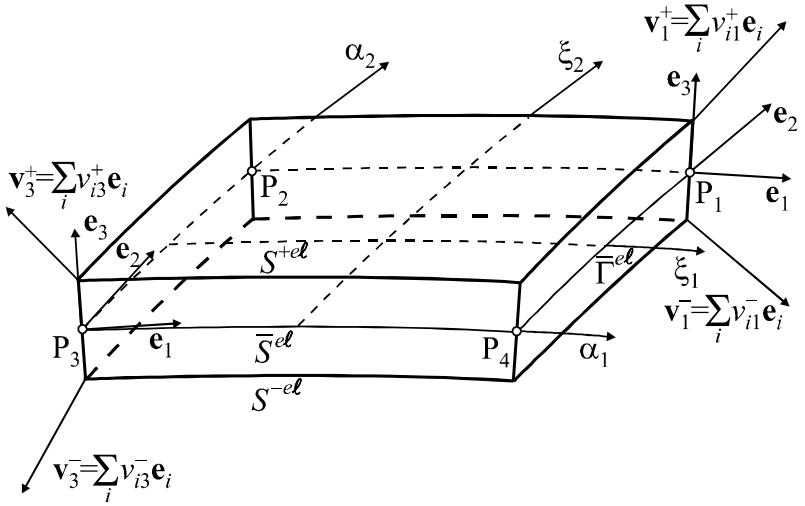

$\mathrm{P}_1\left(\alpha_1^{+e\ell},\alpha_2^{+e\ell}\right)$, $\mathrm{P}_2\left(\alpha_1^{-e\ell},\alpha_2^{+e\ell}\right)$, $\mathrm{P}_3\left(\alpha_1^{-e\ell},\alpha_2^{-e\ell}\right)$, $\mathrm{P}_4\left(\alpha_1^{+e\ell},\alpha_2^{-e\ell}\right)$ are the nodal points of the element

Figure 2: Four-node ESLT element

4 Finite Element Formulation

For the simplest quadrilateral four-node shell element the displacement field is approximated according to the standard C^0 interpolation

$$\mathbf{v}=\sum_r N_r\left(\xi_1,\xi_2\right)\mathbf{v}_r,\qquad \mathbf{v}_r=\left[v_{1r}^-\ v_{1r}^+\ v_{2r}^-\ v_{2r}^+\ v_{3r}^-\ v_{3r}^+\right]^{\mathrm{T}}, \qquad (23)$$

where $\mathbf{v}_r$ are the displacement vectors of the element nodes; $N_r(\xi_1, \xi_2)$ are the linear shape functions of the element; the index $r = \overline{1,4}$ denotes a number of nodes. The load vector is also assumed to vary linearly inside the element.

In a result, for the displacement-dependent strains (3) we have the following approximation:

$$\mathbf{e} = \sum_{r_1, r_2} \xi_1^{r_1} \xi_2^{r_2} \mathbf{e}^{r_1 r_2}, \qquad \mathbf{e}^{r_1 r_2} = \mathbf{B}^{r_1 r_2} \mathbf{V}, \tag{24}$$

$$\mathbf{e}^{r_1 r_2} = \left[e_{11}^{-r_1 r_2} \;\; e_{11}^{+r_1 r_2} \;\; e_{22}^{-r_1 r_2} \;\; e_{22}^{+r_1 r_2} \;\; 2e_{12}^{-r_1 r_2} \;\; 2e_{12}^{+r_1 r_2} \;\; 2e_{13}^{-r_1 r_2} \;\; 2e_{13}^{+r_1 r_2} \;\; 2e_{23}^{-r_1 r_2} \;\; 2e_{23}^{+r_1 r_2} \;\; e_{33}^{r_1 r_2} \right]^{\mathrm{T}},$$

$$\mathbf{V} = \left[\mathbf{v}_1^{\mathrm{T}} \;\; \mathbf{v}_2^{\mathrm{T}} \;\; \mathbf{v}_3^{\mathrm{T}} \;\; \mathbf{v}_4^{\mathrm{T}} \right]^{\mathrm{T}},$$

where $\mathbf{V}$ is the displacement vector at nodal points of the element; $\mathbf{B}^{r_1 r_2}$ are the matrices of order 11×24 corresponding to the strain-displacement transformation. Throughout this section superscripts r_1, r_2 take the values 0 and 1.

To avoid shear and membrane locking and have no spurious zero energy modes, the assumed strain and stress resultant fields inside the element are introduced [5]

$$\mathbf{E} = \sum_{r_1, r_2} \xi_1^{r_1} \xi_2^{r_2} \mathbf{Q}^{r_1 r_2} \mathbf{E}^{r_1 r_2}, \tag{25a}$$

$$\mathbf{E}^{00} = \left[E_{11}^{-00} \; E_{11}^{+00} \; E_{22}^{-00} \; E_{22}^{+00} \; 2E_{12}^{-00} \; 2E_{12}^{+00} \; 2E_{13}^{-00} \; 2E_{13}^{+00} \; 2E_{23}^{-00} \; 2E_{23}^{+00} \; E_{33}^{00} \right]^{\mathrm{T}}, \; \mathbf{E}^{11} = \left[E_{33}^{11} \right],$$

$$\mathbf{E}^{01} = \left[E_{11}^{-01} \; E_{11}^{+01} \; 2E_{13}^{-01} \; 2E_{13}^{+01} \; E_{33}^{01} \right]^{\mathrm{T}}, \; \mathbf{E}^{10} = \left[E_{22}^{-10} \; E_{22}^{+10} \; 2E_{23}^{-10} \; 2E_{23}^{+10} \; E_{33}^{10} \right]^{\mathrm{T}},$$

$$\mathbf{H} = \sum_{r_1, r_2} \xi_1^{r_1} \xi_2^{r_2} \mathbf{Q}^{r_1 r_2} \mathbf{H}^{r_1 r_2}, \tag{25b}$$

$$\mathbf{H}^{00} = \left[H_{11}^{-00} \; H_{11}^{+00} \; H_{22}^{-00} \; H_{22}^{+00} \; H_{12}^{-00} \; H_{12}^{+00} \; H_{13}^{-00} \; H_{13}^{+00} \; H_{23}^{-00} \; H_{23}^{+00} \; H_{33}^{00} \right]^{\mathrm{T}}, \; \mathbf{H}^{11} = \left[H_{33}^{11} \right],$$

$$\mathbf{H}^{01} = \left[H_{11}^{-01} \; H_{11}^{+01} \; H_{13}^{-01} \; H_{13}^{+01} \; H_{33}^{01} \right]^{\mathrm{T}}, \; \mathbf{H}^{10} = \left[H_{22}^{-10} \; H_{22}^{+10} \; H_{23}^{-10} \; H_{23}^{+10} \; H_{33}^{10} \right]^{\mathrm{T}},$$

$$\mathbf{Q}^{01} = \begin{bmatrix} 1 & 0 & 0 & 0 & 0 \\ 0 & 1 & 0 & 0 & 0 \\ 0 & 0 & 0 & 0 & 0 \\ 0 & 0 & 0 & 0 & 0 \\ 0 & 0 & 0 & 0 & 0 \\ 0 & 0 & 0 & 0 & 0 \\ 0 & 0 & 1 & 0 & 0 \\ 0 & 0 & 0 & 1 & 0 \\ 0 & 0 & 0 & 0 & 0 \\ 0 & 0 & 0 & 0 & 0 \\ 0 & 0 & 0 & 0 & 1 \end{bmatrix}, \quad \mathbf{Q}^{10} = \begin{bmatrix} 0 & 0 & 0 & 0 & 0 \\ 0 & 0 & 0 & 0 & 0 \\ 1 & 0 & 0 & 0 & 0 \\ 0 & 1 & 0 & 0 & 0 \\ 0 & 0 & 0 & 0 & 0 \\ 0 & 0 & 0 & 0 & 0 \\ 0 & 0 & 0 & 0 & 0 \\ 0 & 0 & 0 & 0 & 0 \\ 0 & 0 & 1 & 0 & 0 \\ 0 & 0 & 0 & 1 & 0 \\ 0 & 0 & 0 & 0 & 1 \end{bmatrix}, \quad \mathbf{Q}^{11} = \begin{bmatrix} 0 \\ 0 \\ 0 \\ 0 \\ 0 \\ 0 \\ 0 \\ 0 \\ 0 \\ 0 \\ 1 \end{bmatrix}, \tag{25c}$$

where $\mathbf{Q}^{00}$ is the identity matrix of order 11×11; $\mathbf{E}^{00}$ and $\mathbf{H}^{00}$ are the vectors of homogeneous states of strains and stress resultants; $\mathbf{E}^{01}$, $\mathbf{E}^{10}$, $\mathbf{E}^{11}$ and $\mathbf{H}^{01}$, $\mathbf{H}^{10}$, $\mathbf{H}^{11}$ are the vectors of higher approximation modes of strains and stress resultants.

Note that this approach may be treated as a hybrid stress-strain formulation and was proposed by Wempner et al. [21] for the Timoshenko-Mindlin-type shells without the thickness change. Further developments for the Timoshenko beam, Mindlin plate and Timoshenko-Mindlin-type shell theories with account for the thickness strain can be found in works [22-24]. Herein, the more general approach based on the ESL shell theory is presented.

Substituting approximations (23)-(25) into mixed variational equation (22) and using the standard variational procedure, one derives governing equations of the developed finite element formulation

$$\mathbf{E}^{r_1 r_2} = \left(\mathbf{Q}^{r_1 r_2}\right)^{\mathrm{T}} \mathbf{B}^{r_1 r_2} \mathbf{V}, \qquad \mathbf{H}^{r_1 r_2} = \left(\mathbf{Q}^{r_1 r_2}\right)^{\mathrm{T}} \mathbf{D}\mathbf{Q}^{r_1 r_2} \mathbf{E}^{r_1 r_2}, \tag{26}$$
$$\sum_{\mathrm{r}_1, r_2} \frac{1}{3^{\mathrm{r}_1 + r_2}} \left(\mathbf{B}^{r_1 r_2}\right)^{\mathrm{T}} \mathbf{Q}^{r_1 r_2} \mathbf{H}^{r_1 r_2} = \mathbf{F},$$

where **F** is the force vector.

Eliminating further strains and stress resultants from equations (26), we arrive at the element equilibrium equations

$$\mathbf{K}\mathbf{V} = \mathbf{F}, \tag{27}$$

where **K** is the elemental stiffness matrix defined as

$$\mathbf{K} = \sum_{r_1, r_2} \frac{1}{3^{r_1 + r_2}} \left(\mathbf{B}^{r_1 r_2}\right)^{\mathrm{T}} \mathbf{Q}^{r_1 r_2} \left(\mathbf{Q}^{r_1 r_2}\right)^{\mathrm{T}} \mathbf{D}\mathbf{Q}^{r_1 r_2} \left(\mathbf{Q}^{r_1 r_2}\right)^{\mathrm{T}} \mathbf{B}^{r_1 r_2}. \tag{28}$$

4.1 Remark Regarding Linking Equations

The transverse shear and normal displacement-independent strains satisfy the following coupling conditions:

$$hE_{33}^{10} = 2\overline{A}_1^{e\ell}\left(E_{13}^{+00} - E_{13}^{-00}\right), \qquad hE_{33}^{11} = 2\overline{A}_1^{e\ell}\left(E_{13}^{+01} - E_{13}^{-01}\right), \tag{29}$$
$$hE_{33}^{01} = 2\overline{A}_2^{e\ell}\left(E_{23}^{+00} - E_{23}^{-00}\right), \qquad hE_{33}^{11} = 2\overline{A}_2^{e\ell}\left(E_{23}^{+10} - E_{23}^{-10}\right).$$

A proof of this statement is given in work [20].

Coupling equations (29) play a central role in our finite element formulation because they imply that only 18 assumed strain modes are *independent* of 22 modes from approximation (25a). In a result, the elemental stiffness matrix (28) has six, and only six, zero eigenvalues as required for satisfaction of the general rigid-body motion representation, since 24 displacement degrees of freedom are introduced. It should be mentioned that our elemental stiffness matrix requires only direct substitutions, i.e., no inversion is needed if sides of the element coincide with the lines of principal curvatures of the reference surface. Furthermore, it is evaluated by using the full exact *analytical* integration. So, our finite element formulation is very economical and efficient compared to the conventional isoparametric finite element formulations because it eliminates the costly numerical integration by deriving the elemental stiffness matrices [25, 26].

4.2 Remark Concerning Analytical Integration

During the analytical integration the following schemes are employed for computing strains from relationships (4) and (5):

$$e_{\alpha\alpha}^{\pm}=\left\{\frac{1}{\zeta_{\alpha}^{\pm}}\right\}^{00}\sum_{r_1,r_2}\xi_1^{r_1}\xi_2^{r_2}\lambda_{\alpha}^{\pm r_1 r_2},\quad 2e_{12}^{\pm}=\sum_{r_1,r_2}\xi_1^{r_1}\xi_2^{r_2}\left[\left\{\frac{1}{\zeta_1^{\pm}}\right\}^{00}\omega_1^{\pm r_1 r_2}+\left\{\frac{1}{\zeta_2^{\pm}}\right\}^{00}\omega_2^{\pm r_1 r_2}\right], \quad (30)$$

$$2e_{\alpha 3}^{\pm}=\sum_{r_1,r_2}\xi_1^{r_1}\xi_2^{r_2}\left[\left\{\frac{\zeta_{\alpha}^{\pm}}{\overline{\zeta}_{\alpha}}\right\}^{00}\beta_{\alpha}^{r_1 r_2}-\left\{\frac{1}{\overline{\zeta}_{\alpha}}\right\}^{00}\theta_{\alpha}^{\pm r_1 r_2}\right],\qquad e_{33}=\sum_{r_1,r_2}\xi_1^{r_1}\xi_2^{r_2}\beta_3^{r_1 r_2},$$

where

$$\lambda_{\alpha}^{\pm r_1 r_2}=\left\{\frac{1}{A_{\alpha}^{e\ell}}v_{\alpha}^{\pm}\right\}_{\alpha}^{r_1 r_2}+\left\{B_{\alpha\alpha}^{e\ell}v_{\alpha}^{\pm}+B_{\alpha\beta}^{e\ell}v_{\beta}^{\pm}+k_{\alpha}v_3^{\pm}\right\}^{r_1 r_2}, \quad (31)$$

$$\omega_{\alpha}^{\pm r_1 r_2}=\left\{\frac{1}{A_{\alpha}^{e\ell}}v_{\beta}^{\pm}\right\}_{\alpha}^{r_1 r_2}+\left\{B_{\alpha\alpha}^{e\ell}v_{\beta}^{\pm}-B_{\alpha\beta}^{e\ell}v_{\alpha}^{\pm}\right\}^{r_1 r_2}\quad(\beta\neq\alpha),$$

$$\theta_{\alpha}^{\pm r_1 r_2}=-\left\{\frac{1}{A_{\alpha}^{e\ell}}v_3^{\pm}\right\}_{\alpha}^{r_1 r_2}+\left\{-B_{\alpha\alpha}^{e\ell}v_3^{\pm}+k_{\alpha}v_{\alpha}^{\pm}\right\}^{r_1 r_2},\qquad \beta_i^{r_1 r_2}=\frac{1}{h}\left\{v_i^{+}-v_i^{-}\right\}^{r_1 r_2}.$$

In formulas (30) and (31) in accordance with Figure 2 convenient mesh notations are used

$$\{f\}^{00}=\frac{1}{4}\left[f(P_1)+f(P_2)+f(P_3)+f(P_4)\right],\quad \{f\}^{01}=\frac{1}{4}\left[f(P_1)+f(P_2)-f(P_3)-f(P_4)\right],$$

$$\{f\}^{10}=\frac{1}{4}\left[f(P_1)-f(P_2)-f(P_3)+f(P_4)\right],\quad \{f\}^{11}=\frac{1}{4}\left[f(P_1)-f(P_2)+f(P_3)-f(P_4)\right],$$

$$\{f\}_1^{00}=\{f\}^{10},\qquad \{f\}_1^{01}=\{f\}^{11},\qquad \{f\}_1^{10}=\{f\}_1^{11}=0, \quad (32)$$

$$\{f\}_2^{00}=\{f\}^{01},\qquad \{f\}_2^{10}=\{f\}^{11},\qquad \{f\}_2^{01}=\{f\}_2^{11}=0.$$

As concerned a product $\overline{A}_1^{e\ell}\overline{A}_2^{e\ell}$ from variational equation (22), it does not vary inside the element and with account for notation (32) the simplest approximation is employed

$$\overline{A}_1^{e\ell}\overline{A}_2^{e\ell}=\left\{\overline{A}_1^{e\ell}\overline{A}_2^{e\ell}\right\}^{00}.$$

5 Numerical Tests

To assess the accuracy and effectiveness of the developed four-node ESLT element, three standard benchmark problems were employed. They are a three-layer angle-ply plate, a pinched isotropic cylindrical shell and a pinched three-layer cross-ply hyperbolic shell.

5.1 Cylindrical Bending of Three-Layer Angle-Ply Plate

Consider a problem of cylindrical bending of the simply supported angle-ply plate subjected to the sinusoidally distributed pressure load. This problem has been chosen for numerical testing the anisotropic plate response [27], since all components of the displacement vector are different from zero but independent on α_2 coordinate. The geometrical and material data of the three-layer plate are given in Figure 3, where subscripts L and T refer to the fiber and transverse directions of the individual ply; γ is measured in the clockwise direction from α_1 to the fiber direction.

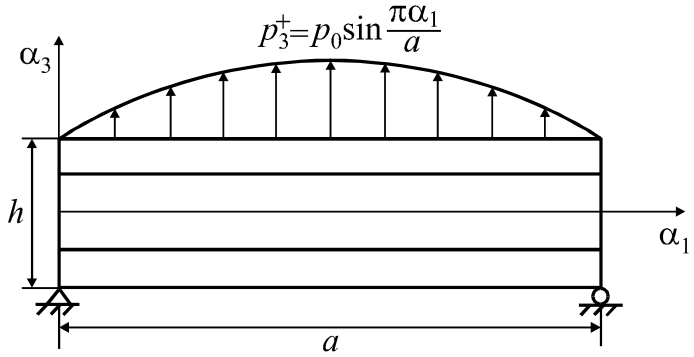

$$h_0 = h/4\,,\ \gamma = 30^\circ\,,\ E_{\mathrm{L}} = 2.5\times10^7\,,\ E_{\mathrm{T}} = 10^6$$
$$G_{\mathrm{LT}} = 5\times10^5\,,\ G_{\mathrm{TT}} = 2\times10^5\,,\ \nu_{\mathrm{LT}} = \nu_{\mathrm{TT}} = 0.25$$
$$\text{Ply thicknesses} = [h_0/2h_0/h_0],\ \text{ply orientations} = [\gamma/-\gamma/\gamma]$$

Figure 3: Cylindrical bending of three-layer angle-ply plate

Figure 4 shows the distribution of the dimensionless transverse shear stress in the thickness direction at cross-section $\alpha_1 = 0$ for two values of the slenderness ratio a/h. The transverse components of the stress tensor are computed by integrating the 3D elasticity equations with account for equilibrium conditions at the layer interfaces and boundary conditions on the bottom surface [17, 18]. Due to this approach the boundary conditions for the transverse components on the top surface are also satisfied. It is seen that all results agree closely, especially Pagano's and LWT solutions.

5.2 Pinched Cylindrical Shell with Rigid Diaphragms

To illustrate the capability of the developed four-node ESLT element to overcome membrane and shear locking phenomena and to compare it with high performance four-node quadrilateral elements [28-31], we consider one of the most demanding standard linear tests. A short cylindrical shell supported by two rigid diaphragms at the ends is loaded by two opposite concentrated forces in its middle section. The geometrical and material properties of the shell are shown in Figure 5.

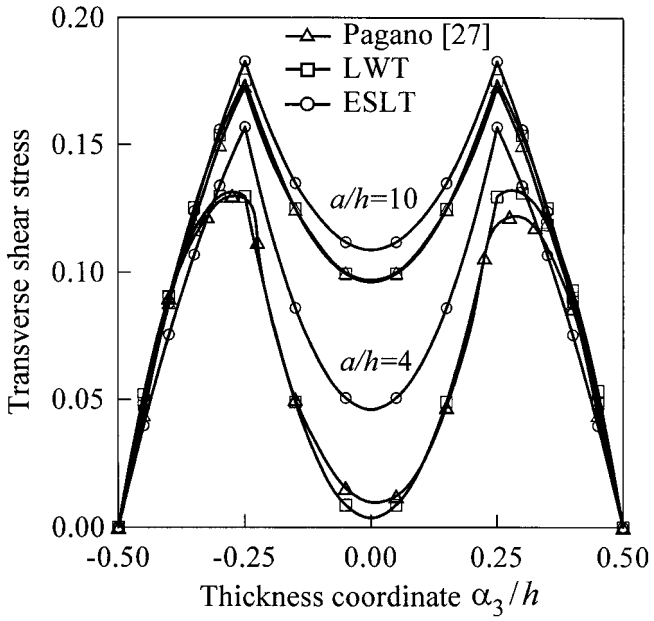

Figure 4: Distribution of transverse shear stress $-\sigma_{23}h/p_0a$ in thickness direction at $\alpha_1 = 0$ of three-layer angle-ply plate

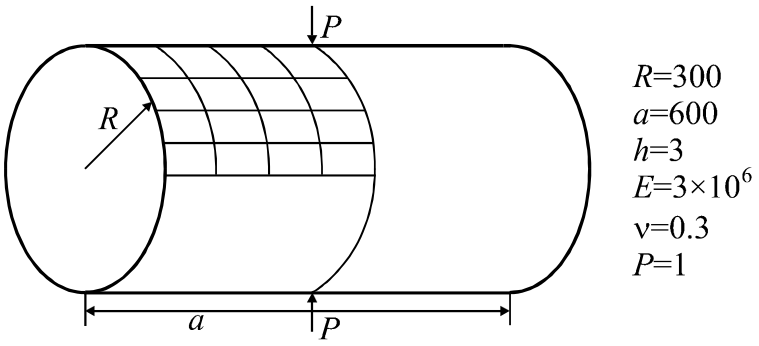

Figure 5: Pinched cylindrical shell with rigid diaphragms

Mesh	Four-node elements				ESLT element
	[28]	[29]	[30]	[31]	
4x4	0.373	0.469	0.370	0.399	0.890
8x8	0.747	0.791	0.740	0.763	0.941
16x16	0.935	0.946	0.930	0.935	0.986

Table 1: Normalized transverse displacement $(\bar{v}_3)^{\text{Norm}}$ under applied load of pinched cylindrical shell with rigid diaphragms

Owing to symmetry of the problem, only one octant of the shell is modeled with regular meshes of ESLT elements. Table 1 displays the normalized transverse displacement under the applied load and a comparison with above four-node quadrilateral elements. The displacements are normalized with respect to the analytical solution -1.8248×10^{-5} [32]. As can be seen, our results exhibit an excellent agreement even for coarse meshes.

5.3 Pinched Three-Layer Cross-Ply Hyperbolic Shell

A cross-ply hyperbolic shell under two pairs of opposite concentrated forces was considered by Basar et al. [33] for testing finite deformation formulations for composite shells, while we employ this example as a linear benchmark test to assess the proposed schemes (30)-(32) of the analytical integration. Besides, as in the pinched cylinder example we can verify a proper representation of inextensional bending and, additionally, this is an excellent test for the ability of the element to model rigid-body motions. The geometrical and material data of the three-layer hyperbolic shell are given in Figure 6, where 0° and 90° refer to the circumferential and meridional directions.

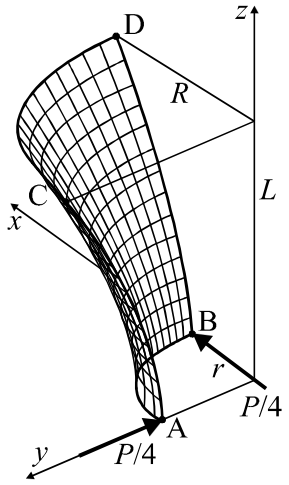

r=7.5
R=15
L=20
h=0.04
$h_0=h/3$
$E_L=4\times10^7$
$E_T=10^6$
$G_{LT}=G_{TT}=6\times10^5$
$\nu_{LT}=\nu_{TT}=0.25$
P=4
Ply thicknesses=[$h_0/h_0/h_0$]
Ply orientations=[0/90/0]

Shell of revolution with geometrical parameters $\left(\alpha_1 = z \in [0, L],\ \alpha_2 \in [0, \pi/2]\right)$:

$$A_1 = \sqrt{1+\frac{\mu^2 z^2}{A_2^2}},\quad A_2 = r\sqrt{1+\frac{\mu z^2}{r^2}},\quad k_1 = -\frac{\mu r^2}{A_1^3 A_2^3},\quad k_2 = \frac{1}{A_1 A_2},\quad \mu = \frac{R^2 - r^2}{L^2}$$

Figure 6: Pinched three-layer cross-ply hyperbolic shell

Due to summery, only one octant of the shell is discretized with uniform meshes of ESLT elements. Table 2 lists normalized displacements at points A, B, C and D. The displacements are normalized with respect to values $-\bar{v}_y^{\mathrm{A}} = \bar{v}_x^{\mathrm{B}} = 0.1013$ and $\bar{v}_y^{\mathrm{C}} = -\bar{v}_x^{\mathrm{D}} = 0.09785$, respectively, where $\bar{v}_x$ and $\bar{v}_y$ denote displacements of the

middle surface in x and y directions. Such values are the computationally exact solutions of this problem based on the consistent mesh refinements. One can observe that the ESLT element performs well.

Mesh	$\left(\bar{v}_y^{\mathrm{A}}\right)^{\mathrm{Norm}}$	$\left(\bar{v}_x^{\mathrm{B}}\right)^{\mathrm{Norm}}$	$\left(\bar{v}_y^{\mathrm{C}}\right)^{\mathrm{Norm}}$	$\left(\bar{v}_x^{\mathrm{D}}\right)^{\mathrm{Norm}}$
2x2	0.5963	0.5963	1.1474	1.1474
4x4	0.8728	0.8728	1.0337	1.0337
8x8	0.9612	0.9612	1.0089	1.0089
16x16	0.9881	0.9881	1.0020	1.0020

Table 2: Normalized displacements at points A, B, C and D of pinched cross-ply hyperbolic shell

6 Conclusion

In this work principally new strain-displacement relationships of the ESL and LW shell theories have been developed. These relationships are very attractive because they are objective, i.e., invariant under all rigid-body motions. So, they may be used for the formulation of effective curved multilayered shell elements in local curvilinear surface coordinates. However, the practical use of such strain-displacement relationships require a development of the constitutive equations, in order to overcome thickness locking phenomena.

The simple and efficient hybrid stress-strain four-node curved ESLT element has been formulated. The finite element formulation is based on the original approach in which displacement vectors of the face surfaces are introduced and represented in the local reference surface basis. So, as fundamental unknowns six displacements of the face surfaces and, additionally, 11 strains and 11 conjugate stress resultants have been chosen. This allows, in particular, special loading conditions at the bottom and top surfaces and shell edges to be accounted for.

The ESLT element developed does not contain any spurious zero energy modes and possesses six zero eigenvalues. It is important that the elemental stiffness matrix requires only direct substitutions (no inversion is needed) and it is evaluated by using the full exact analytical integration. Therefore, our formulation is very simple and economical compared to conventional isoparametric formulations.

References

[1] A.L. Gol'denveiser, “Theory of Elastic Thin Shells”, Pergamon Press, Oxford, 1961.

[2] G. Cantin, “Strain Displacement Relationships for Cylindrical Shells”, AIAA Journal, 6, 1787-1788, 1968.

[3] D.J. Dawe, “Rigid-Body Motions and Strain-Displacement Equations of Curved Shell Finite Elements”, International Journal of Mechanical Sciences,

14, 569-578, 1972.
[4] G.M. Kulikov, S.V. Plotnikova, “Efficient Mixed Timoshenko-Mindlin Shell Elements”, International Journal for Numerical Methods in Engineering, 55, 1167-1183, 2002.
[5] G.M. Kulikov, S.V. Plotnikova, “Simple and Effective Elements Based upon Timoshenko-Mindlin Shell Theory”, Computer Methods in Applied Mechanics and Engineering, 191, 1173-1187, 2002.
[6] E.I. Grigolyuk, G.M. Kulikov, “Multilayered Reinforced Shells: Analysis of Pneumatic Tires”, Mashinostroyenie, Moscow, 1988 (in Russian).
[7] J.N. Reddy, “Mechanics of Laminated Composite Plates: Theory and Analysis”, CRC Press, Boca Raton, FL, 1997.
[8] E.I. Grigolyuk, G.M. Kulikov, “General Direction of Development of the Theory of Multilayered Shells”, Mechanics of Composite Materials, 24, 231-241, 1988.
[9] A.K. Noor, W.S. Burton, “Assessment of Computational Models for Multilayered Composite Shells”, Applied Mechanics Reviews, 43(4), 67-97, 1990.
[10] E. Carrera, “Theories and Finite Elements for Multilayered, Anisotropic, Composite Plates and Shells", Archives of Computational Methods in Engineering, 9, 1-60, 2002.
[11] E. Carrera, “Historical Review of Zig-Zag Theories for Multilayered Plates and Shells”, Applied Mechanics Reviews, 56(3), 287-308, 2003.
[12] G.M. Kulikov, “Non-Linear Analysis of Multilayered Shells under Initial Stress”, International Journal of Non-Linear Mechanics, 36, 323-334, 2001.
[13] M.F. Ausserer, S.W. Lee, “An Eighteen-Node Solid Element for Thin Shell Analysis”, International Journal for Numerical Methods in Engineering, 26, 1345-1364, 1988.
[14] H.C. Park, C. Cho, S.W. Lee, “An Efficient Assumed Strain Element Model with Six DOF per Node for Geometrically Nonlinear Shells”, International Journal for Numerical Methods in Engineering, 38, 4101-4122, 1995.
[15] K.Y. Sze, S. Yi, M.H. Tay, “An Explicit Hybrid Stabilized Eighteen-Node Solid Element for Thin Shell Analysis”, International Journal for Numerical Methods in Engineering, 40, 1839-1856, 1997.
[16] K.Y. Sze, “Three-Dimensional Continuum Finite Element Models for Plate/Shell Analysis”, Progress in Structural Engineering and Materials, 4, 400-407, 2002.
[17] G.M. Kulikov, “Analysis of Initially Stressed Multilayered Shells”, International Journal of Solids and Structures, 38, 4535-4555, 2001.
[18] G.M. Kulikov, “Refined Global Approximation Theory of Multilayered Plates and Shells”, Journal of Engineering Mechanics, 127, 119-125, 2001.
[19] K. Washizu, “Variational Methods in Elasticity and Plasticity”, 3rd ed., Pergamon Press, Oxford, 1982.
[20] G.M. Kulikov, S.V. Plotnikova, “Equivalent Single-Layer and Layer-Wise Shell Theories and Rigid-Body Motions - Part I: Foundations”, Mechanics Advanced Materials Structures, submitted.
[21] G. Wempner, D. Talaslidis, C.M. Hwang, “A Simple and Efficient Approximation of Shells via Finite Quadrilateral Elements”, Journal of Applied Mechan-

ics, 49, 115-120, 1982.
[22] G.M. Kulikov, S.V. Plotnikova, “Non-Conventional Non-Linear Two-Node Hybrid Stress-Strain Curved Beam Elements”, Finite Elements in Analysis and Design, 27 journal pages, 2004.
[23] G.M. Kulikov, S.V. Plotnikova, “Finite Deformation Plate Theory and Large Rigid-Body Motions”, International Journal of Non-Linear Mechanics, 39, 1093-1109, 2004.
[24] G.M. Kulikov, S.V. Plotnikova, “Non-Linear Strain-Displacement Equations Exactly Representing Large Rigid-Body Motions. Part I. Timoshenko-Mindlin Shell Theory”, Computer Methods in Applied Mechanics and Engineering, 192, 851-875, 2003.
[25] S. Ahmad, B.M. Irons, O.C. Zienkiewicz, “Analysis of Thick and Thin Shell Structures by Curved Shell Elements”, International Journal for Numerical Methods in Engineering, 2, 419-451, 1970.
[26] K.J. Bathe, “Finite Element Procedures”, Prentice Hall, New Jersey, 1996.
[27] N.J. Pagano, “Influence of Shear Coupling in Cylindrical Bending of Anisotropic Laminates”, Journal of Composite Materials, 4, 330-343, 1970.
[28] T.J.R. Hughes W.K. Liu, “Nonlinear Finite Element Analysis of Shells. Part II: Two-Dimensional Shells”, Computer Methods in Applied Mechanics and Engineering, 27, 167-182, 1981.
[29] D. Lam, W.K. Liu, E.S. Law, T. Belytschko, “Resultant-Stress Degenerated-Shell Element”, Computer Methods in Applied Mechanics and Engineering, 55, 259-300, 1986.
[30] K.J. Bathe, E.N. Dvorkin, “A Formulation of General Shell Elements - the Use of Mixed Interpolation of Tensorial Components”, International Journal for Numerical Methods in Engineering, 22, 697-722, 1986.
[31] J.C. Simo, D.D. Fox, M.S. Rifai, “On a Stress Resultant Geometrically Exact Shell Model. Part II: The Linear Theory; Computational Aspects”, Computer Methods in Applied Mechanics and Engineering, 73, 53-92, 1989.
[32] G.R. Heppler, J.S. Hansen, “A Mindlin Element for Thick and Deep Shells”, Computer Methods in Applied Mechanics and Engineering, 54, 21-47, 1986.
[33] Y. Basar, Y. Ding, R. Schultz, “Refined Shear-Deformation Models for Composite Laminates with Finite Rotations”, International Journal of Solids and Structures, 30, 2611-2638, 1993.